Space-time variation of the Typhoon Morkat (2009) rainband structure over Taiwan's complex terrain observed by weather radars and rain gauge measurements

廖宇慶　陳台琦　蔡宜君
唐玉霜　林沛練　李永安

Department of Atmospheric Sciences
National Central University, Taiwan

Outline:

(1) Introduction.

(2) Rain band structure revealed by radar reflectivity.

(3) Precipitation distribution revealed by rain gauge observations.

(4) 3-D wind structure retrieved by a new multiple-Doppler radar wind analysis method.

(5) Summary and future work.

- Morakot (2009) produced ~3,000 mm / 4 days rainfall, triggered severe mudslides and flooding in southern Taiwan.

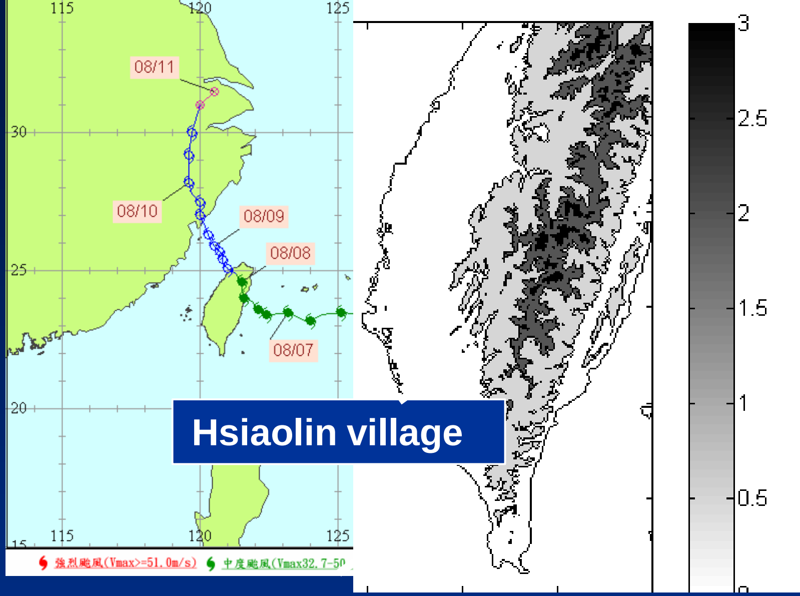

- Convergence of the typhoon circulation and SW monsoon flow.
- Slow moving speed after landfall (~ 5 km/hr).
- Terrain effect.
- Asymmetric latent heat release.

(Lee et al. 2011, Chien and Kuo 2011, Wang et al. 2012)

1. To study the structure and evolution of the typhoon rainband.
2. To understand the orographic effect on the rainfall distribution.

Data source

- Taiwan Central Weather Bureau (CWB)
  - S-band Doppler radar (RCCG)
  - Rain gauges

- Taiwan Air Force
  - C-band dual-pol./Doppler radar (RCMK)

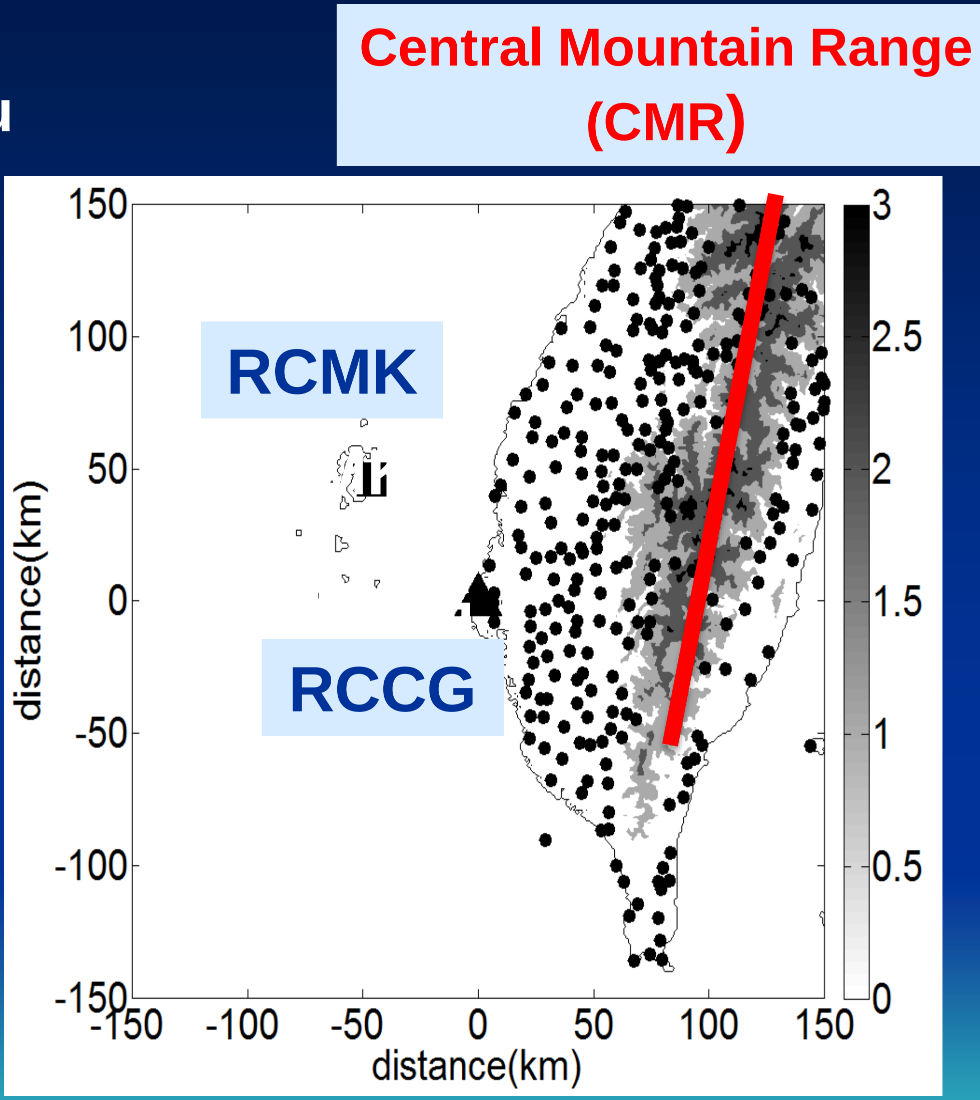

Rainband structure and evolution revealed by radar reflectivity.

Time-space plots Z=3km

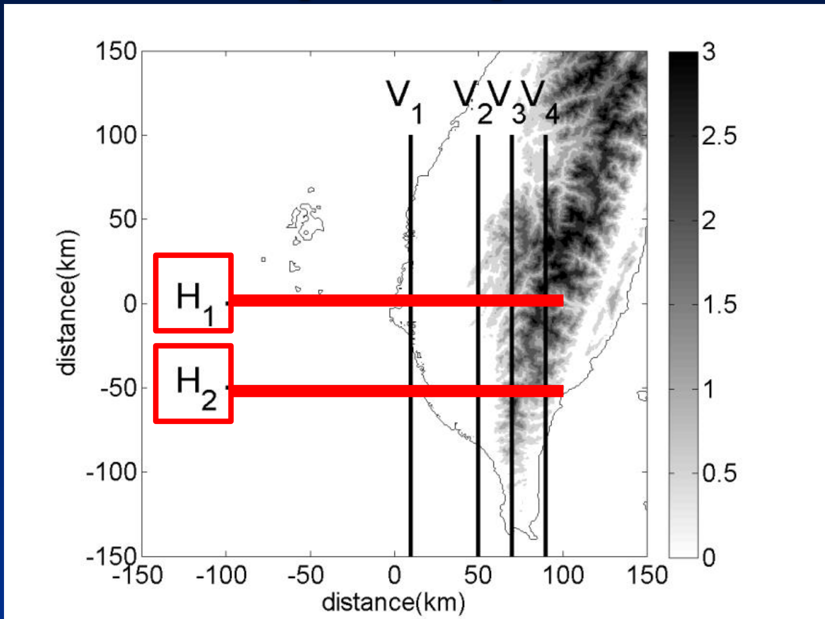

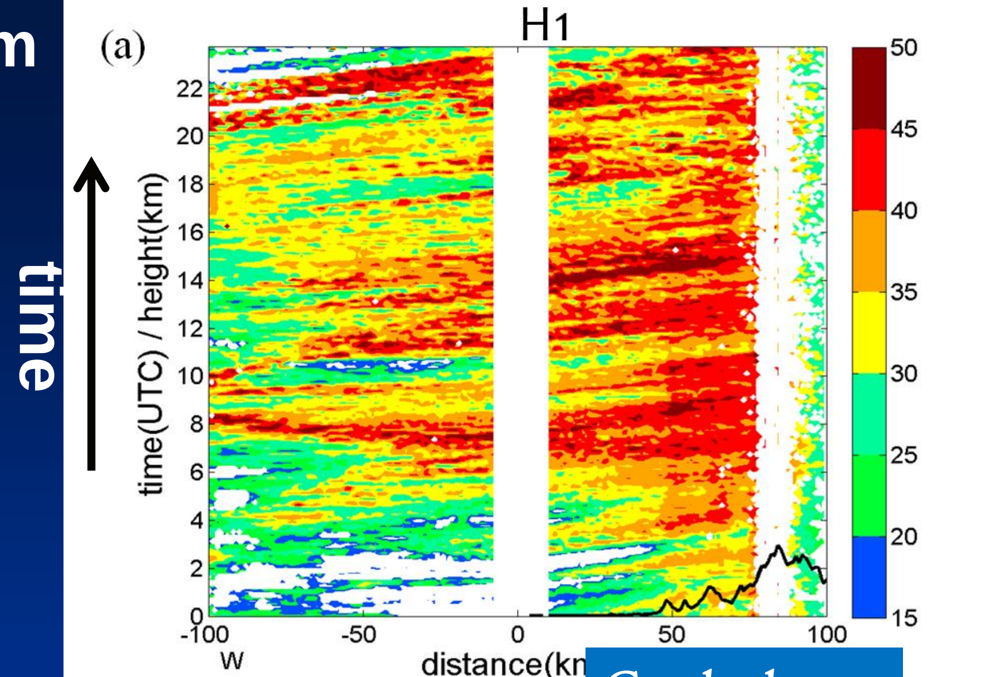

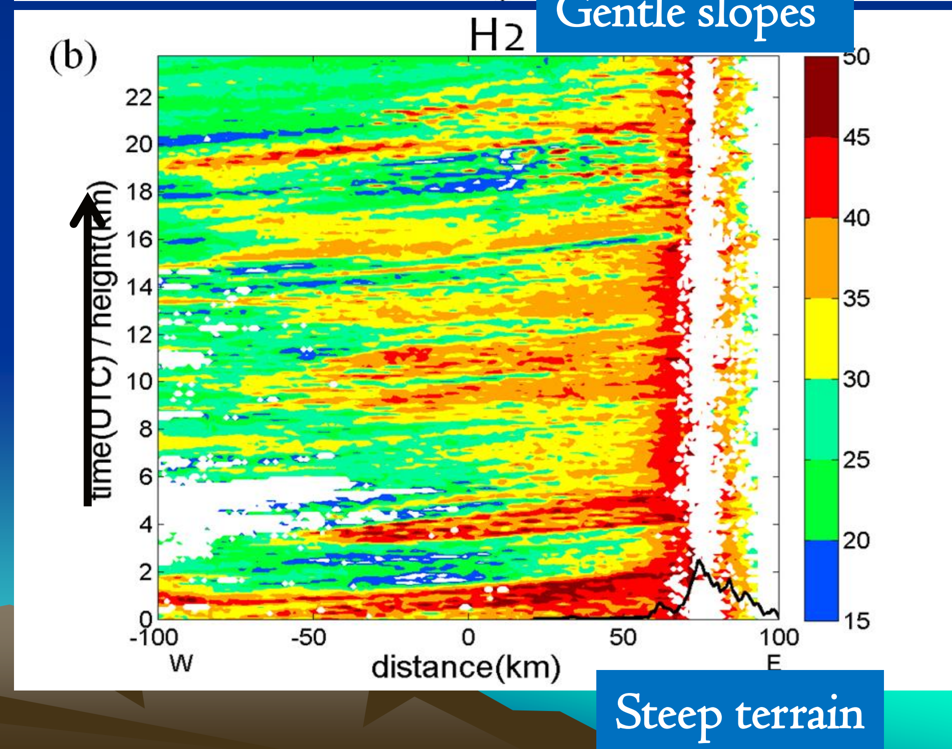

In the north (H1), cells moved from ocean, intensify/enlarge, before reaching CMR.

In the south (H2), cells intensify abruptly in front of steep terrain.

Strong reflectivity seldom extends to the leeside of CMR.

Time-space plot near coastal area

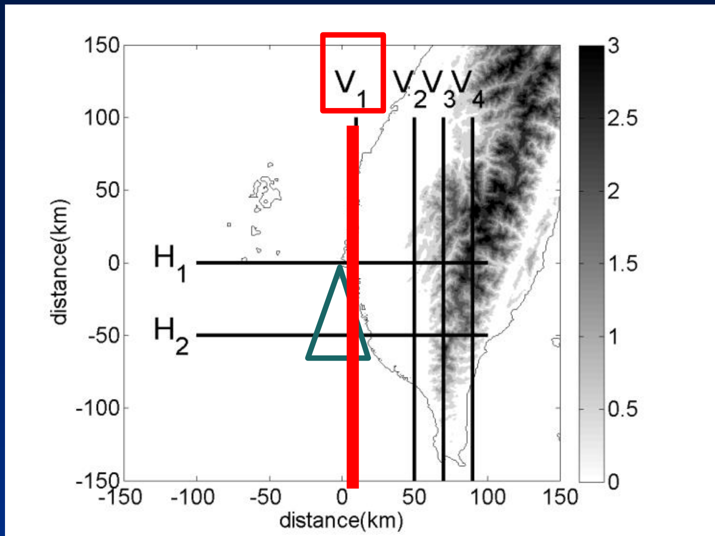

N-S oscillation D~100 km, P~ 8 hr. When prevailing wind is southerly (northerly), rainband moves northward (southward).

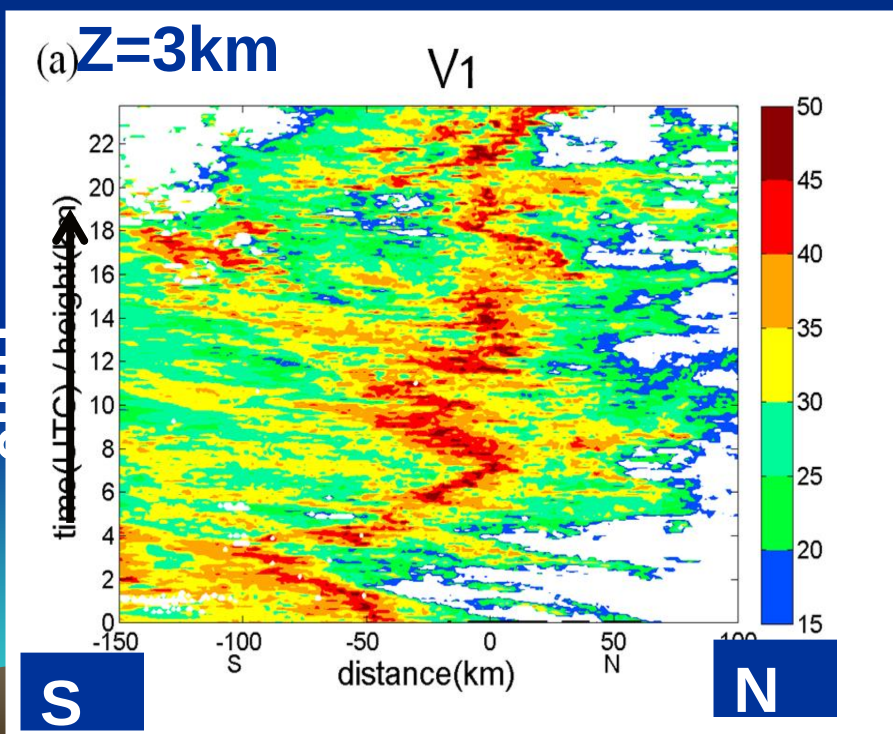

Avg. radial wind south of RCCG

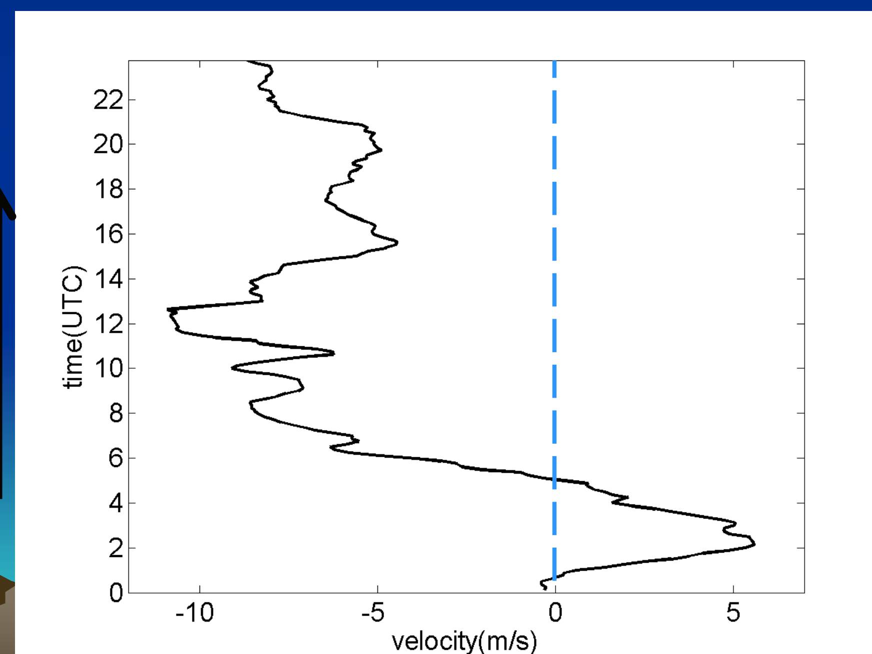

southerly **northerly**

Time-space plot over the foothill

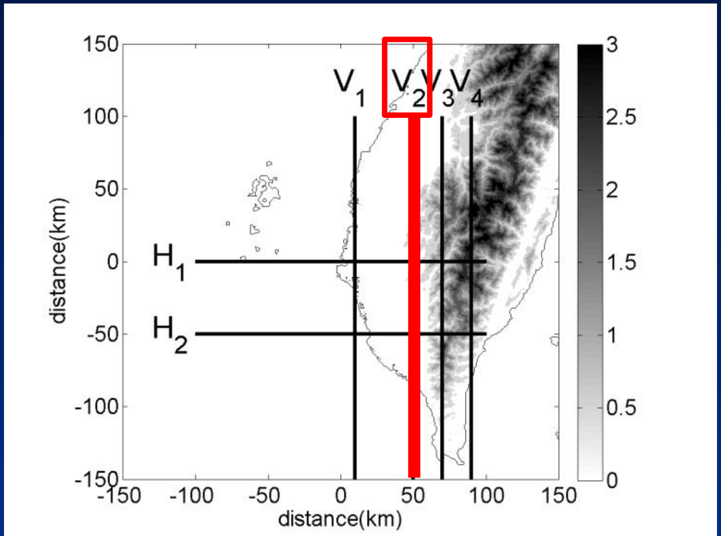

The reflectivity extends its range over the northern portion of foothill

Z=3km

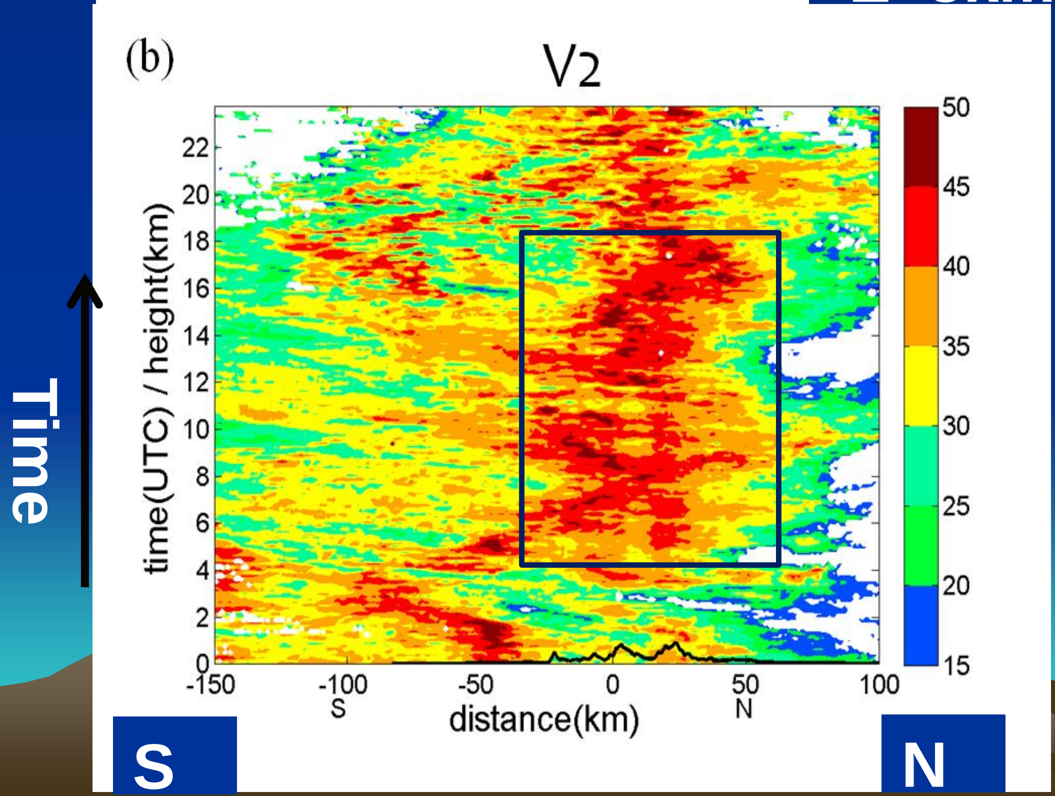

Time-space plot over mountain and peak

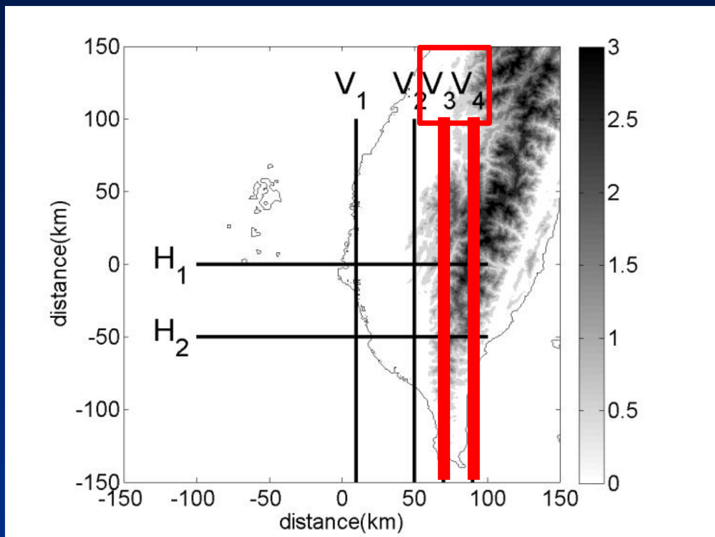

Reflectivity covers large area over CMR along V3, implying heavy precipitation spreads and persists for 24 hours.

Over V4, reflectivity drops dramatically at the peak.

Z=4km V3

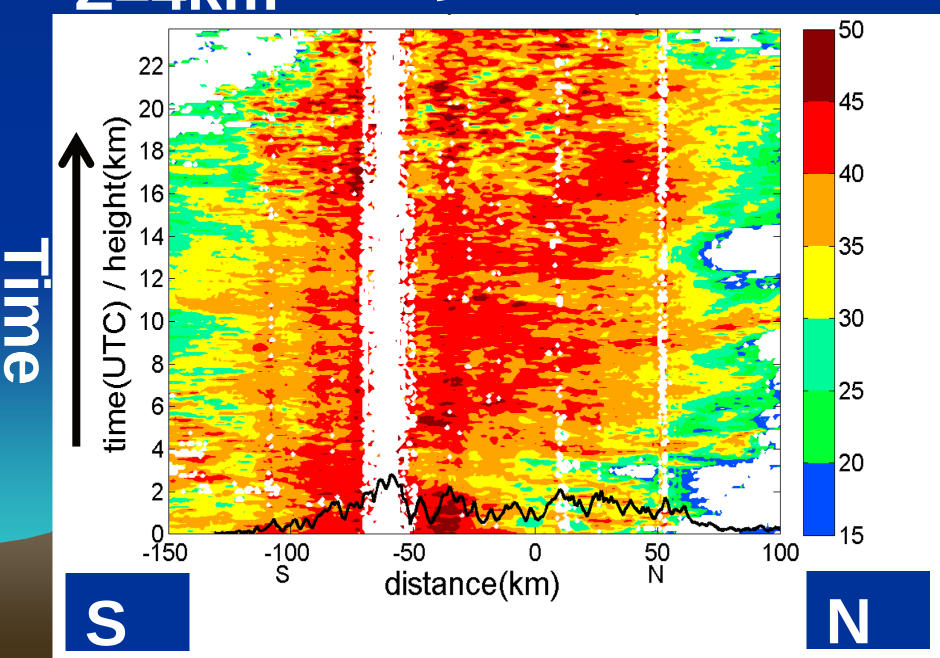

Z=4km V4

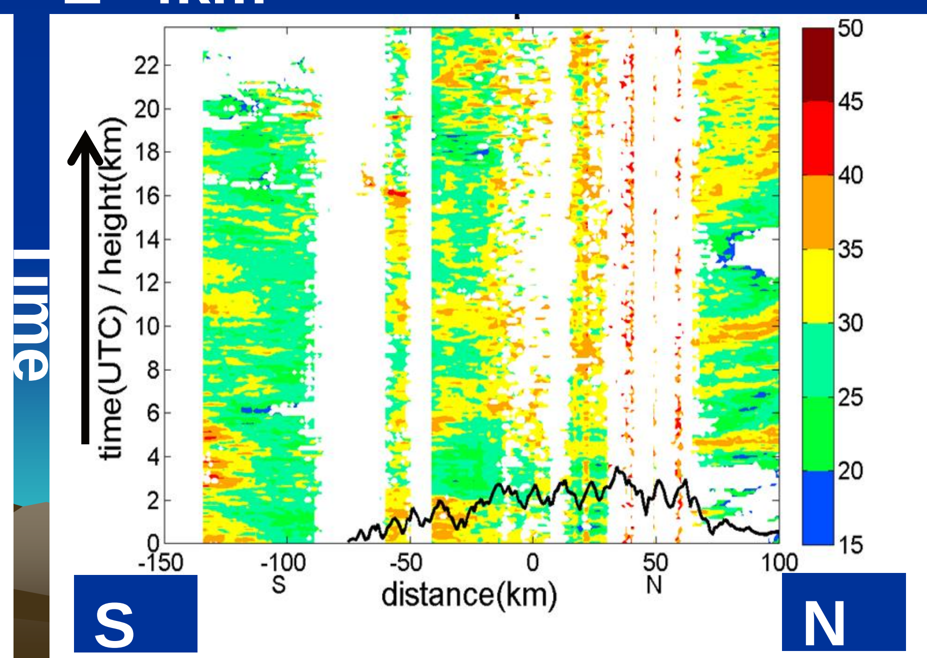

Precipitation pattern revealed by rain gauge observations.

Rain gauge observation in windward side

Avg. hourly rainfall rate (histogram) and accumulated precipitation (solid curve in mm) during 16 UTC 05 Aug to 16 UTC 10 Aug.

- Lesser precipitation over the coastal plain area (Z < 0.2 km). Accumulated rainfall increases substantially when closing CMR (~ 900 mm, 1,600 mm, 1,800 mm, 1,950 mm)

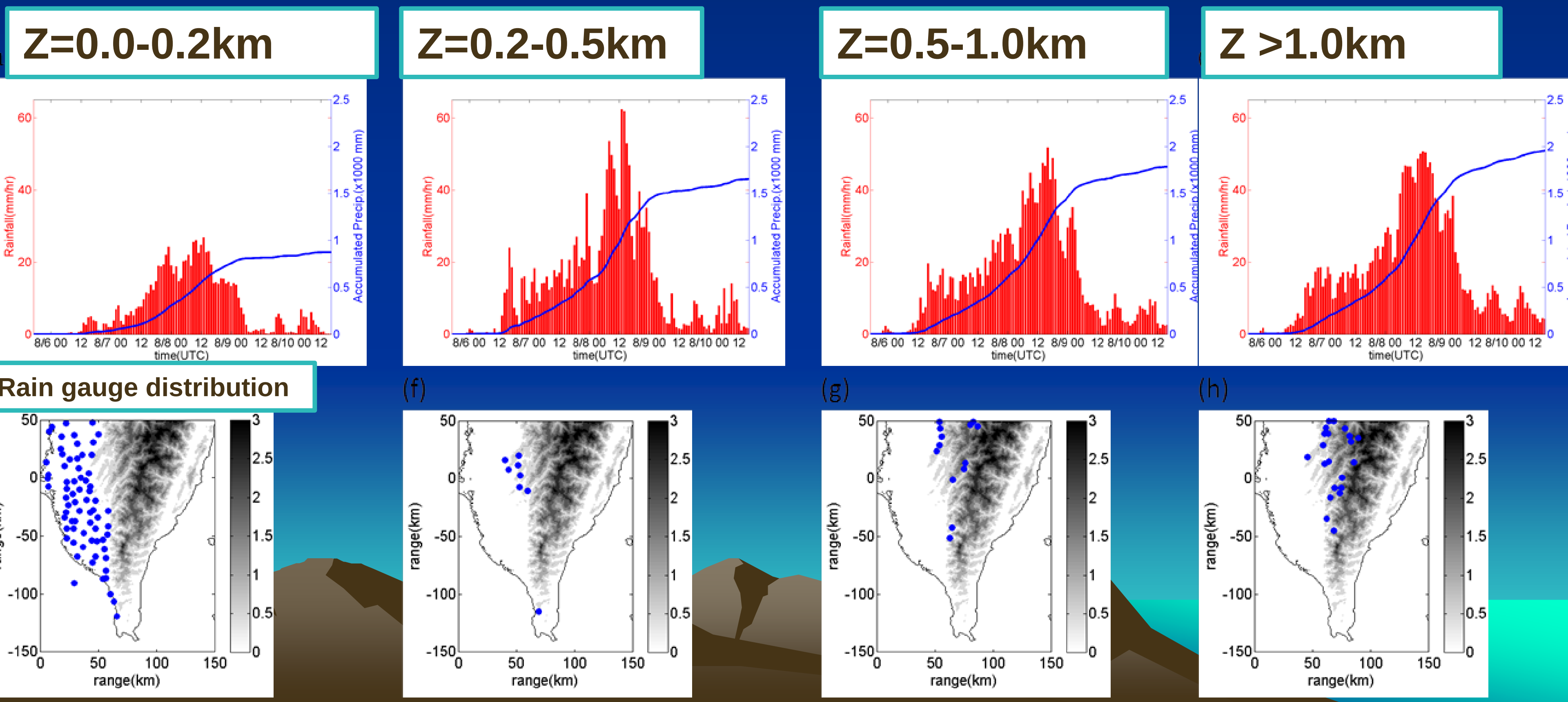

Rain gauge observation in leeward side

- Compared to windward side, the rainfall in leeward side starts **12 hr later**, and ends at least **24 hr earlier**.
- Gauges at Z > 1.0 km observed higher rainfall intensity and amount.
- Both the rainfall intensity and cumulative amount drop dramatically in the leeward side of CMR. (< 30% of the windward side).

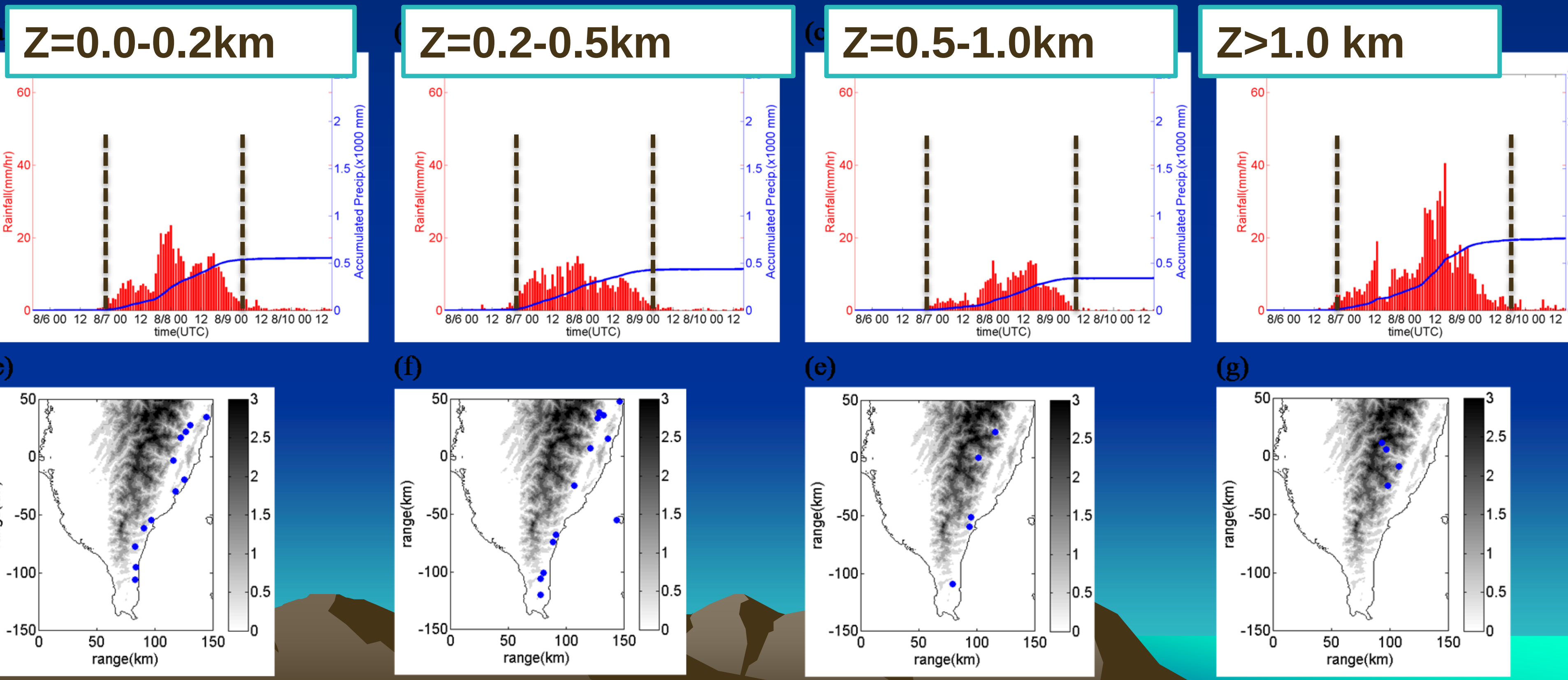

Atmospheric stability (Durran and Klemp 1982) saturated B-V frequency

$$N_{sat}^{\ 2} = g\left\{\frac{1+(Lq_s/RT)}{1+(\varepsilon L^2 q_s/c_p RT^2)} \times \left(\frac{d\ln\theta}{dz} + \frac{L}{c_pT}\frac{dq_s}{dz}\right) - \frac{dq_w}{dz}\right\}$$

$\varepsilon = 0.622$; L: latent heat of evaporation

R: gas constant, T: temperature

q_s : saturation mixing ratio

c_p: specific heat at const. pressure

θ : potential temperature,

q_w: q_s + liquid water mixing ratio

$N_{sat}^{\ 2} < 0 \;\Rightarrow$ unstable

Upslope triggering

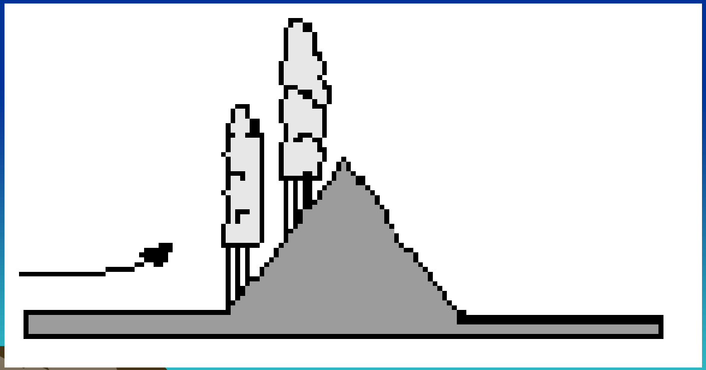

Houze(1993)

3-D wind field in the Morakot rainband retrieved by a new multiple-Doppler wind synthesis method.

Some of the advantages of this new method

1) Easily add any number of radars.

2) Can synthesize wind fields along radar base line.

3) Retrieved 3D wind can be used directly for vorticity budget analysis.

4) Can retrieve winds over complex terrain.

3-D Wind field at Z=1.25km

reflectivity/wind field

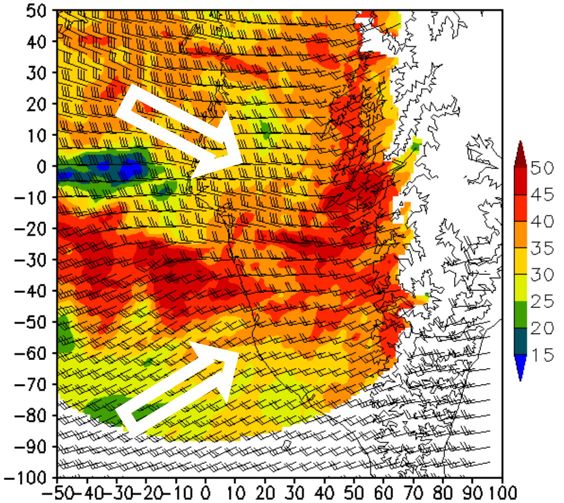

w

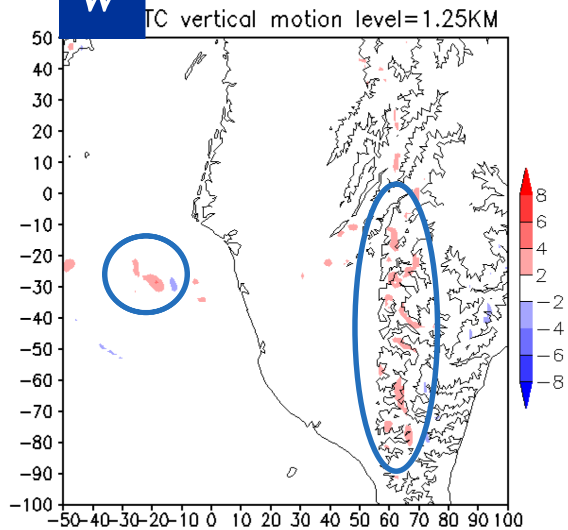

vertical vorticity $\varsigma = \frac{\partial v}{\partial x} - \frac{\partial u}{\partial y}$

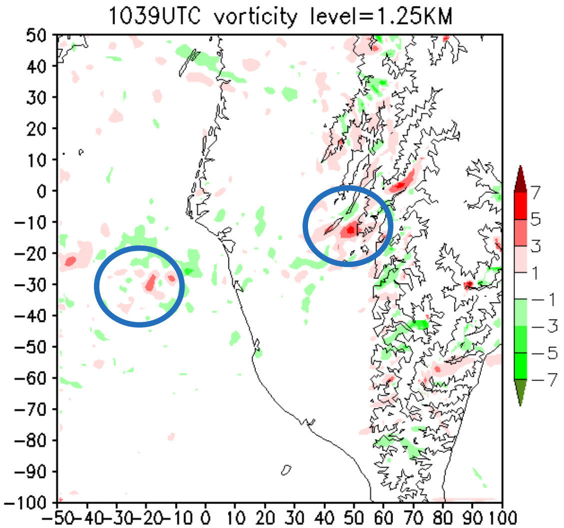

Wind speed

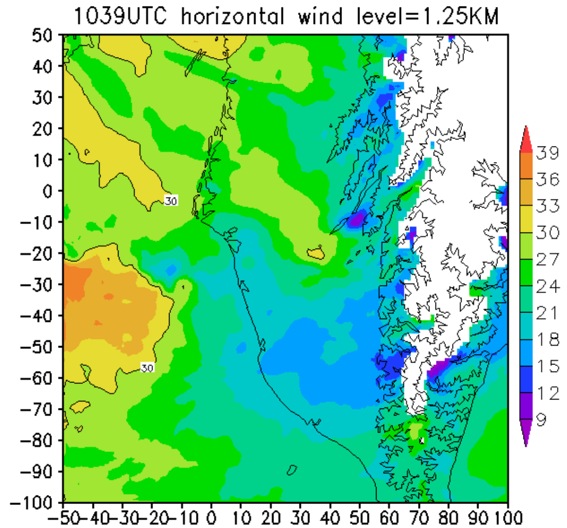

NW flow from the Morakot's circulation converges with the SW flow, strengthen the rainband.

Strong updraft (~ 4 m/s) and positive vertical vorticity in the rain band and near the terrain.

Strong wind speed (> 36 m/s) in the rainband, but drops 50% over land.

3-D Wind field at Z=3.25km

Reflectivity/wind field

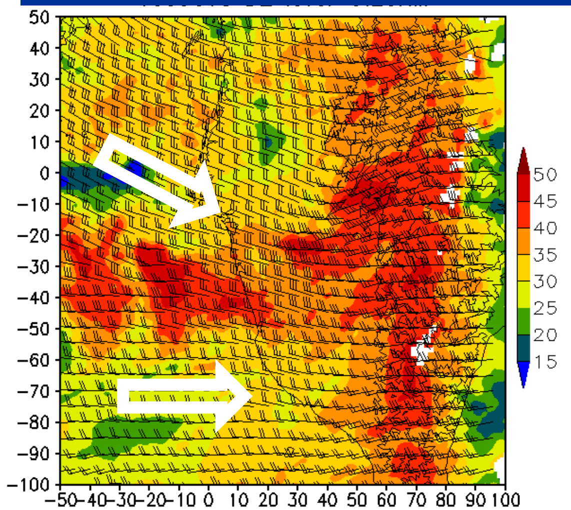

w

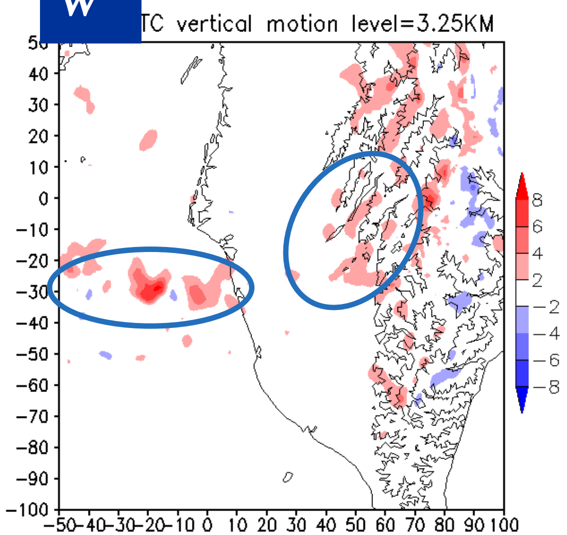

Vertical vorticity $\varsigma = \frac{\partial v}{\partial x} - \frac{\partial u}{\partial y}$

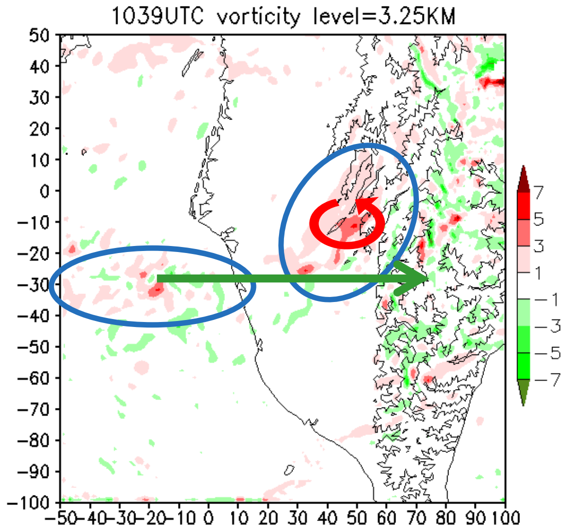

Wind speed

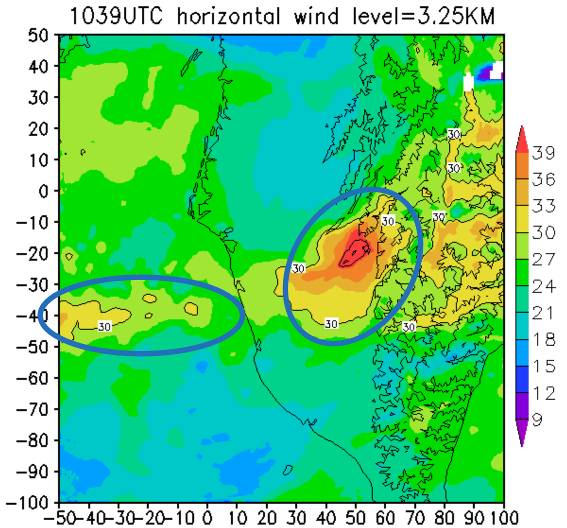

Dominant wind is NW flow from Morakot circulation.

Even stronger updraft (~ 8 m/s) and vorticity in rainband and near CMR.

Vorticity produced mainly by advection , but tilting is also significant.

Wind speed drops at coast, increases rapidly to 40 m/s near the foothill

3-D Wind field at Z=5.75km (> CMR)

Reflectivity/wind field

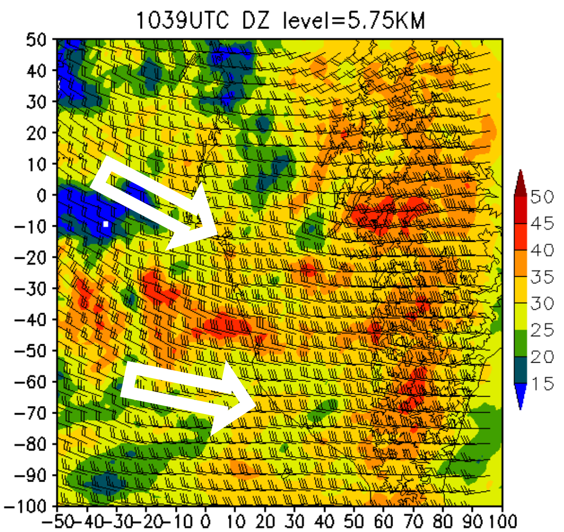

w

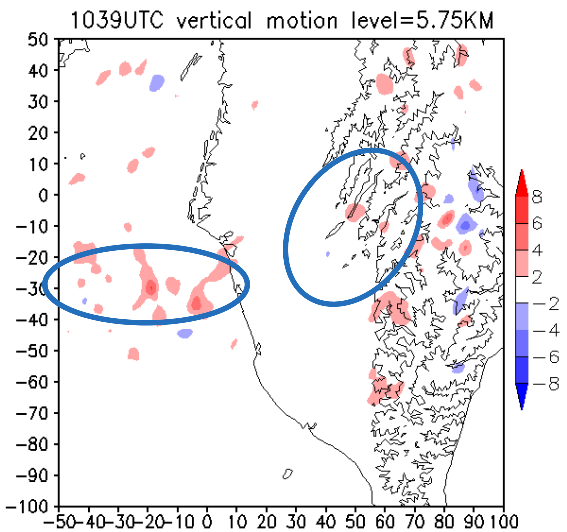

Vertical vorticity $\varsigma = \frac{\partial v}{\partial x} - \frac{\partial u}{\partial y}$

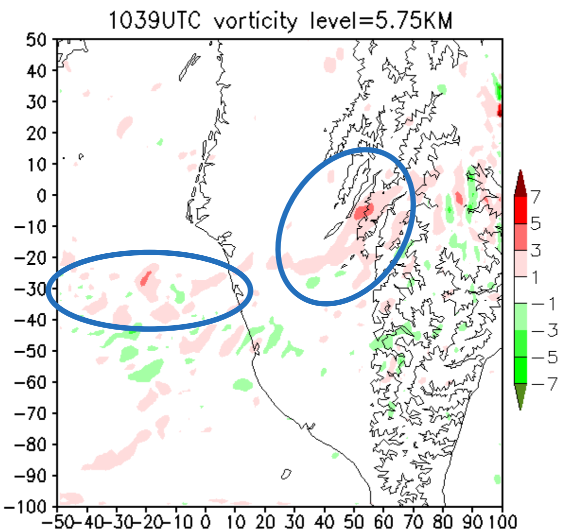

Wind speed

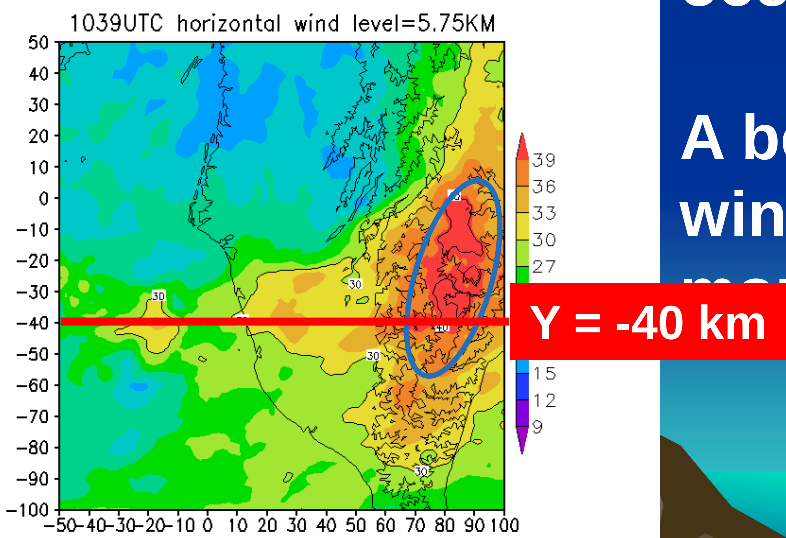

- Dominated by typhoon circulation.

  Strong updraft (~ 6 m/s) and vorticity still exist in the rainband over ocean.

  A belt of strong wind above mountain crest

Retrieved winds along Y = -40 km

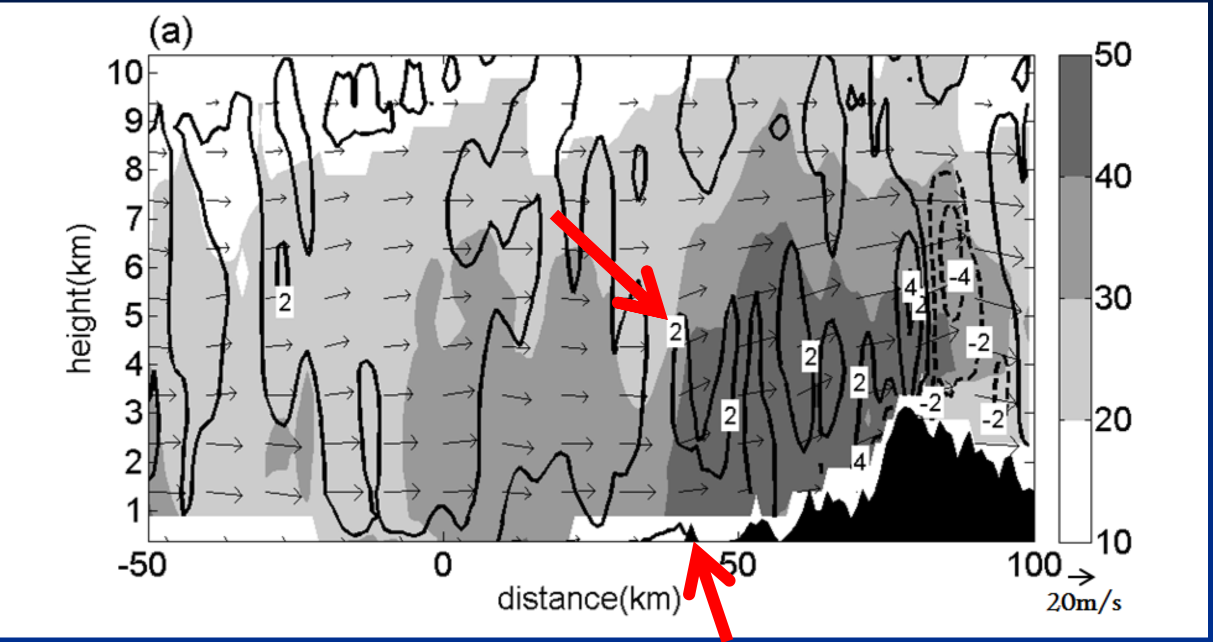

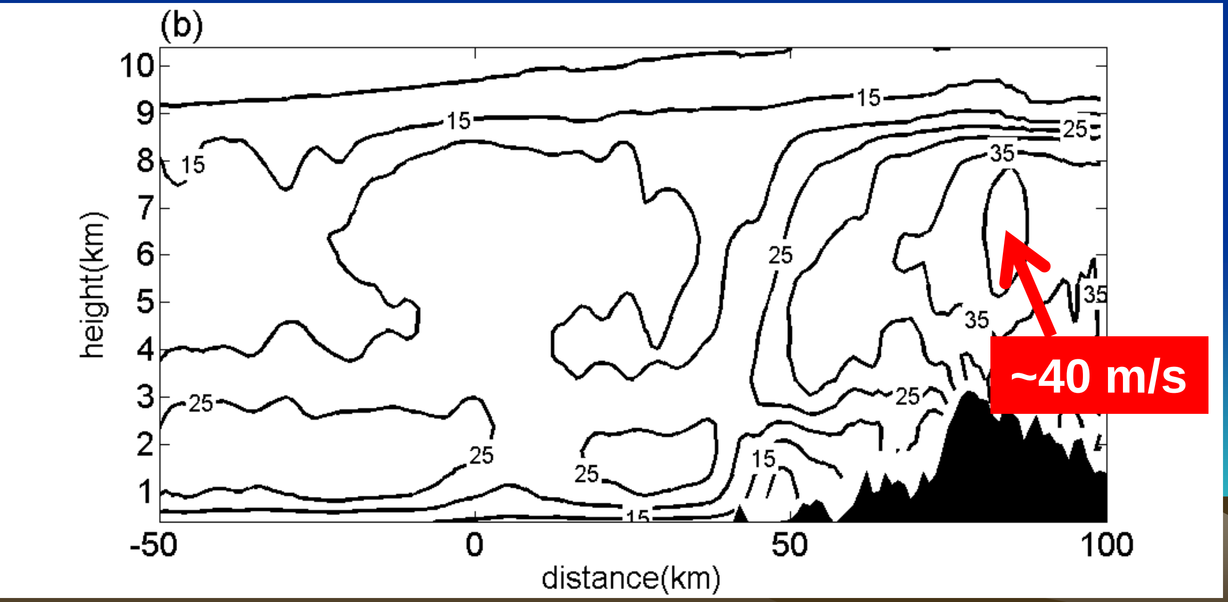

The u-w wind field, radar reflectivity, and w.

Updraft (downdraft) in the windward/lee side of CMR.

Reflectivity starts to intensify when touching terrain.

The cross-barrier wind (u). A wind speed maximum above the mountain. Why ?

$$N_{sat}^{2} < 0 \quad \Rightarrow \quad \textbf{unstable}$$

Strong mixing makes the atmosphere more barotropic, suitable to apply a simplified 2-D shallow-water model.

$$(1 - F_r^2)\frac{\partial u}{\partial x} = \frac{ug}{C^2}\frac{\partial H}{\partial x}$$

$$C^2 = g(h - H)$$

$$F_r^2 = \frac{u^2}{C^2}$$

***u*: cross barrier wind speed**

H: terrain height

h: depth of the underlying barotropic atmosphere.

***C*: Shallow water gravity wave phase speed.**

Fr: shallow water Froud number

$$C^2 = g(h - H)$$

u ~ 20 m/s H ~ 2,000 m

h > H C > u

Fr < 1.0

subcritical condition

(Durran 1986)

$$F_r^2 = \frac{u^2}{C^2}$$

$$\underline{(1 - F_r^2)}\frac{\partial u}{\partial x} = \frac{ug}{\underline{C^2}}\frac{\partial H}{\partial x}$$

> 0

> 0

$\frac{\partial u}{\partial x} > 0$ **as** $\frac{\partial H}{\partial x} > 0$

u **reaches max. as** $\frac{\partial H}{\partial x} = 0$

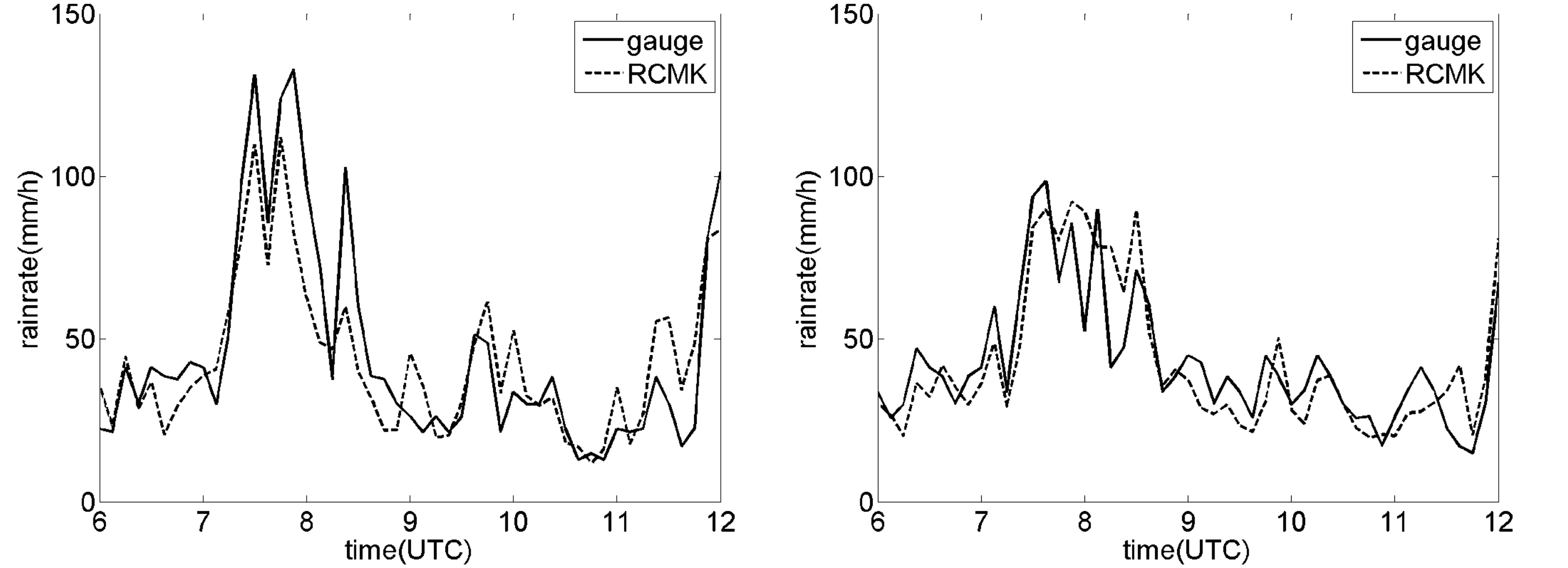

Rainfall rates (mm hr^{-1}) during 06-12 UTC 8 August observed by gauges (solid line) and RCMK (dashed line) at: (left) a low altitude (210 m MSL) site; and (right) a mountain (1,160 m MSL) site.

Summary of Morakot rainband+future work

1) Highly unstable atmosphere, convections triggered/intensify by topographic lifting. Moisture consumed in windward side, causing much lesser rainfall in the leeside.

2) Rainfall intensity and amount increase with height.

3) Rainband shows oscillation over the ocean, but becomes quasi-stationary, and spreads to wide area over the land.

Summary and future work (continue)

4) SW flow converges with typhoon circulation, helps rainband development and its movement toward CMR.

5) Wind speed reaches a maximum above the mountain peak, can be explained by a simplified shallow water model.

6) The RCMK dual-pol radar demonstrates its ability in providing accurate QPE.

7) Use thermodynamic retrieval to understand the temperature/pressure structures. Use dual-polarimetric radar data to study the micro-physical process in the rainband.

Wind synthesis of Typhoon Fanapi (2010) using 7 radars

(RCWF,RCHL,RCKT,RCCG RCMK,RCCK,TEAMR)

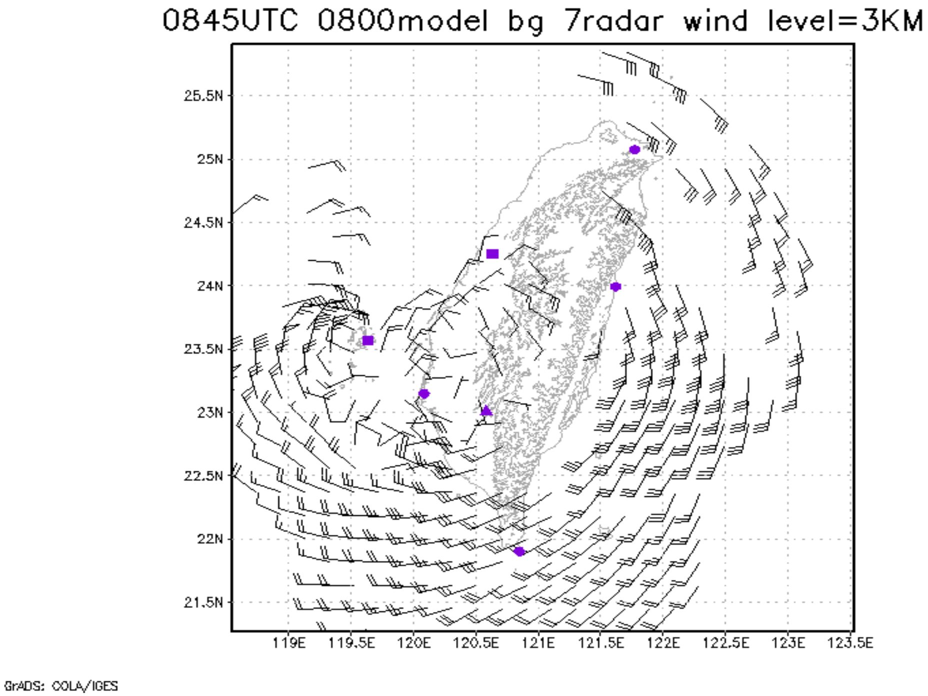

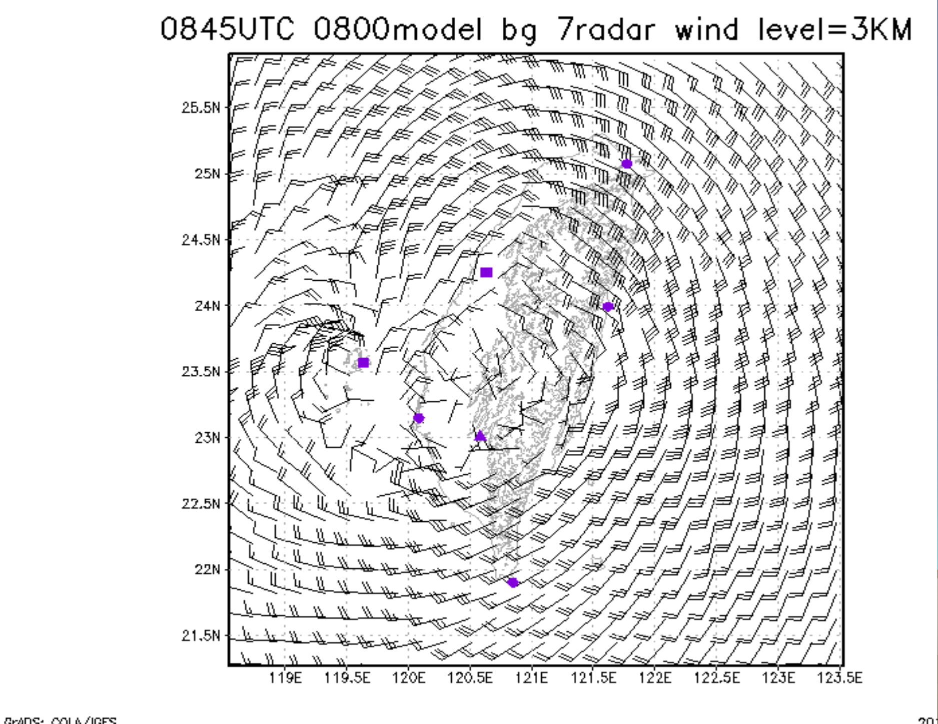

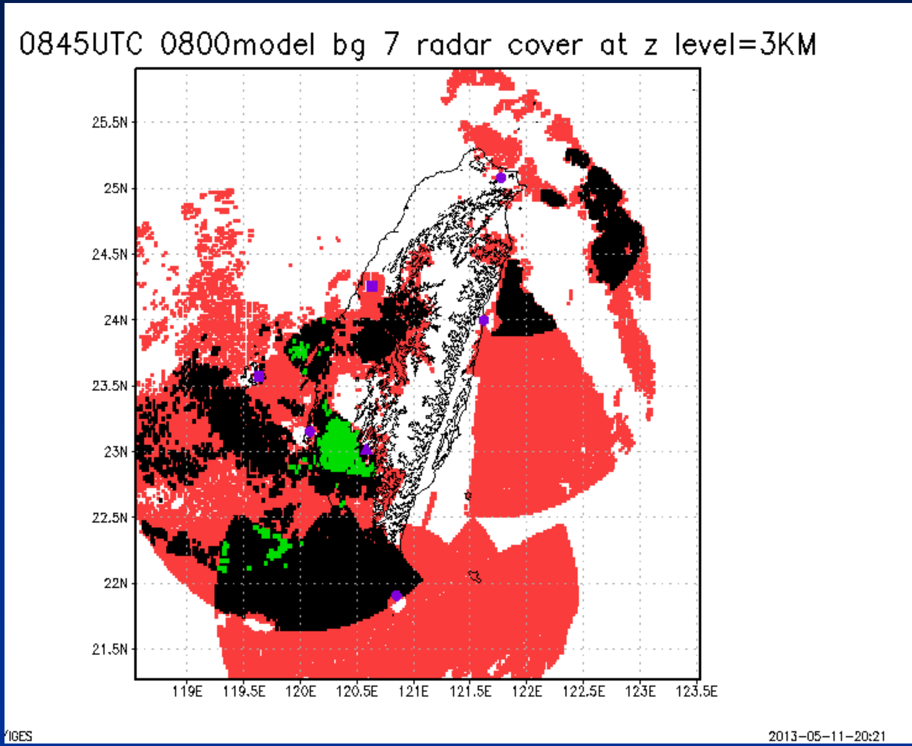

one radar : red
two radars : black
three radars : green

Thank you !